0013-4651/2004/151(2)/A260/5/$7.00 © The Electrochemical Society, Inc.

Alkaline Fuel Cell with Intrinsic Energy Storage

Chunsheng Wang,[a,*,z] A. John Appleby,[b,*] and David L. Cocke[c,*]

[a]*Center for Manufacturing Research and Department of Chemical Engineering, Tennessee Technological University, Cookeville, Tennessee 38505, USA*
[b]*Center for Electrochemical Systems and Hydrogen Research, Texas Engineering Experiment Station, Texas A&M University, College Station, Texas 77843-3402, USA*
[c]*Gill Chair of Chemistry and Chemical Engineering, Lamar University, Beaumont, Texas 77710, USA*

A new high peak power density alkaline fuel cell (FC) was fabricated using a metal hydriding (MH) alloy as the anode electrocatalyst and manganese dioxide as the cathode electrocatalyst. The high-loading MH and MnO_2 electrocatalysts not only gave a satisfactory steady-state power output, but also deliver additional power stored in the charged MH and MnO_2 electrodes when the overall cell voltage fell. Moreover, the MH/MnO_2 FC can still deliver a certain amount of energy even after the hydrogen and oxygen are shut off. The discharged MH and MnO_2 electrodes are recharged by hydrogen and oxygen in the FC when the cell voltage returns to normal levels. This MH/MnO_2 alkaline FC performs the same functions as those of a more complex fuel cell/battery hybrid system with lower weight, volume, and cost.
 [DOI: 10.1149/1.1640627]

Manuscript submitted April 9, 2003; revised manuscript received August 19, 2003. Available electronically January 8, 2004.

Alkaline fuel cells (AFCs) show promise as environmentally friendly electrochemical power sources for distributed cogeneration for building, and transportation applications. As with other FCs, the continuous power output of AFCs is satisfactory, however, their response to instantaneous power load requirements may often be insufficient. To meet such peak power requirements, the AFC must be hybridized with a second battery, a supercapacitor, or both. Normally, AFC/battery/supercapacitor systems use separate components connected by an electrical control system. This results in increased complexity, weight, volume, and cost. One solution is to incorporate a battery element into the FC, *e.g.*, using energy storage materials as electrocatalysts in the electrodes. Such electrode materials should have a high energy storage capacity and have good electrocatalytic activity for anodic hydrogen oxidation and cathodic oxygen reduction.

Metal hydride (MH) alloys and manganese dioxide are excellent electrocatalysts for hydrogen oxidation and oxygen reduction, respectively. In fact, the generic electrolyte-resistant AB_5 alloys, whose parent material is $LaNi_5$, have been successfully used as anode catalyst in AFCs,[1-3] and MnO_2 has been evaluated as an electrocatalyst for oxygen reduction in alkaline solution.[4] Hence, selected MH materials and MnO_2 may be used as electrocatalysts in AFCs. On the other hand, hydrogen or proton from water can reversibly be inserted into or be extracted from MH compounds and MnO_2 over the appropriate potential ranges in alkaline solution. Hence, MH anodes and MnO_2 cathodes in alkaline solution may be used as a rechargeable alkaline cell.[5,6] Recent results show that such cells has several advantages, particularly long cycle life under the correct conditions, no memory effect, high capacity, nontoxicity, low self-discharge rate, high performance, and high cost-effectiveness.[6] Therefore, an alkaline FC with high-loading MH compound as the anode electrocatalyst and high-loading MnO_2 as the cathode electrocatalyst may be given the same functions as those of a complex FC/battery hybrid system, with a consequent reduction in system weight, volume, and cost. Compared to the proton exchange membrane fuel cell (PEMFC) and the direct methanol fuel cell (DMFC), an MH/MnO_2 AFC has a potentially lower cost due to less costly electrolyte and non-platinum-metal electrocatalysts. Another advantage of the MH/MnO_2 AFC is that it can deliver a certain energy even after the hydrogen and oxygen supplies are turned off.

This paper describes AFCs with high loading MH anodes and high loading of MnO_2 cathodes for the first time, and reports their performance during continuous and instantaneous loads, even with interrupted fuel and oxidant supply.

Experimental

Preparation of electrodes and cells.—The MH and MnO_2 electrodes consisted of a hydrophobic gas diffusion layer on the gas side and an active electrocatalyst layer facing the electrolyte. The gas diffusion layer was identical for both electrodes, and was prepared by rolling wet-proofed (35 wt % poly(tetrafluoroethylene, PTFE) acetylene black onto nickel mesh, followed by sintering in an oven at 300°C for 15 min. The MH electrocatalyst layer used the lanthanide mischmetal-based (Lm) alloy $LmNi_{4.1}Co_{0.4}Mn_{0.4}Al_{0.3}$ (200 mesh, Japan Metal & Chemicals Co. Ltd), which was first mixed with nickel powder and wet-proofed (60 wt % PTFE) acetylene black in the mass ratio 60:30:4:6 (MH:Ni:C:PTFE). The mixture was mechanically milled for either 10 or 30 min in a SPEX CertiPre model 8000M mixer/mill. Pure ethanol was added to the milled mixture, which was then rolled onto the gas diffusion layer to form into thin-film type MH anode. Electrodes with three different MH loadings (150, 100, 60 mg/cm^2) were prepared by changing the thickness of the active layer. As with Raney nickel electrocatalysts, $LmNi_{4.1}Co_{0.4}Mn_{0.4}Al_{0.3}$ requires an initial activation *i.e.*, electrochemical charge, a process to fracture or remove the oxide film on the alloy surface. To reduce or eliminate activation requirements, $LmNi_{4.1}Co_{0.4}Mn_{0.4}Al_{0.3}$ was also mixed with 0.5 wt % of platinum electrocatalyst in the form of 10 wt % Pt on Vulcan XC72 carbon black (E-TEK, Inc., (Natick, MA). For the cathode, MnO_2 powders (Alfa Johnson Matthey) were first mixed with graphite in the mass ratio of 1:1, and then mechanical milled for either 5 min or 50 h. A 60 wt % PTFE dispersion was then added to the milled mixture to give a mass ratio 45:45:10 (MnO_2:graphite:PTFE). As for the anode, ethanol was added to the milled mixture, which was rolled on the gas diffusion layer to form thin-film cathodes with different MnO_2 loadings (150, 100, and 60 mg/cm^2).

Figure 1 shows the structure of the MH/MnO_2 test cells. The geometrical surface areas of MH and MnO_2 electrodes in contact with 6 M KOH electrolyte was 1.0 cm^2, and the distance between the anode and cathode was 1.0 cm. An Hg/HgO reference electrode was inserted through a small hole in the center plate. The electrolyte was replaced with fresh electrolyte from time to time via a hole in the cell. Nominally atmospheric-pressure hydrogen and oxygen were supplied behind the electrodes at a stoichiometry of 2.0.

To independently determine the performance of MH and MnO_2 electrodes as rechargeable battery electrodes, they were prepared without gas diffusion layers and were each pressed between two nickel-mesh current collectors to form pellets of 2.0 cm^2 geometric

* Electrochemical Society Active Member.
[z] E-mail: cswang@tntech.edu

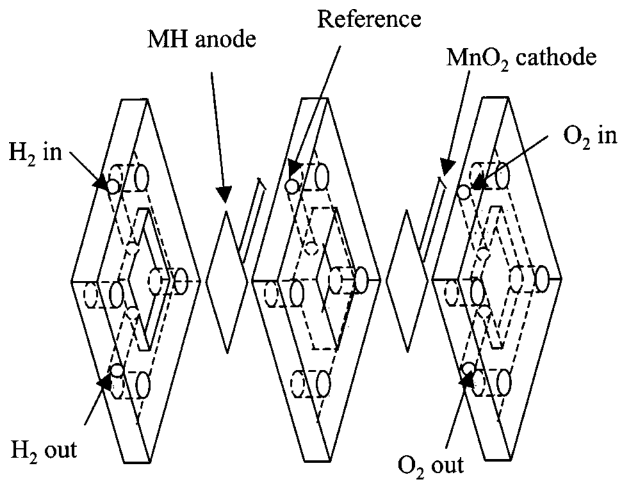

Figure 1. Structure of laboratory MH/MnO_2 AFC.

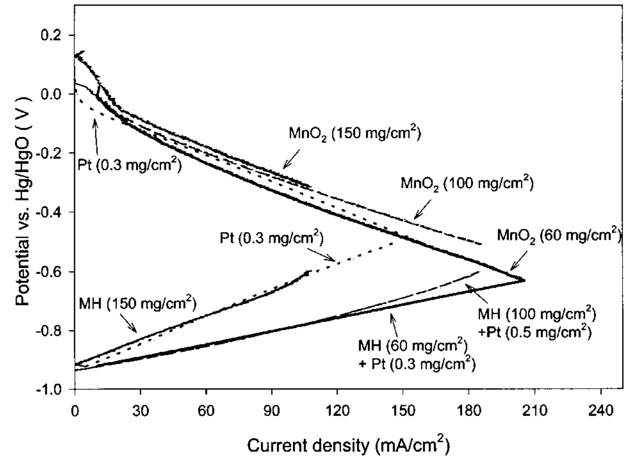

Figure 2. I-E performance of MH ($LmNi_{4.1}Co_{0.4}Mn_{0.4}Al_{0.3}$) anode-$MnO_2$ cathode AFCs as a function of catalyst loading. The performance of an AFC with commercial Zetek Pt/C electrodes (0.3 mg/cm^2 loading) is also shown for comparison. Performance measured by CV at 1.0 mV s^{-1} with H_2 and O_2 as fuel at 25°C.

area and 1.2 mm thickness. The MH or MnO_2 electrodes were placed in the center of a four-compartment glass cell, which had two large area $Ni(OH)_2$/NiOOH electrodes (Hughes Aircraft Company) on either side, and an Hg/HgO reference electrode in the fourth compartment. The 6 M KOH electrolyte was prepared from reagent grade material and deionized (DI) water.

Electrochemical measurement.—The potential-current density (I-E) parameters of test MH/MnO_2 AFCs using hydrogen and oxygen were obtained using cyclic voltammetry (CV) at a scan rate of 1.0 mV/s at room temperature. The electrode potentials were measured *vs.* the Hg/HgO/6M KOH reference electrode at 25°C. All potentials given below are *vs.* this electrode.

The MH electrode without the 0.5 wt % Pt addition was first activated by charging the cell with charge current of 150 mA/g until the potential of MnO_2 reached +0.4 V. This process was repeated five times with a 1.0 h rest period between charges. The catalyst prepared by mechanically milling MH/graphite mixture for 30 min was easily activated because of its fractured oxide film. The electrocatalysts with added Pt develop a sufficiently low open-circuit potential (OCP) in the presence of hydrogen to allow its absorption by $LmNi_{4.1}Co_{0.4}Mn_{0.4}Al_{0.3}$. The resulting volume change rapidly fractures the oxide film, so such electrocatalysts do not require preactivation.

The battery performance of MH and MnO_2 electrodes in 6 M KOH electrolytes was measured by charging MH at a mass current density of 50 mA/g for 6.0 h and charging MnO_2 at the same current to +0.4 V, with discharge under the same current conditions to an end-of-discharge potential of −0.6 V for MH electrodes and −0.7 V for MnO_2 electrode using an Arbin Corporation (College Station, TX) battery cycler.

Electrochemical impedance spectroscopy (EIS) of the MH/MnO_2 FC was measured at OCP, −0.9 and −0.85 V for MH electrodes, and at the OCP, −0.05, −0.1, and −0.15 V for MnO_2 electrodes in the frequency range 65 KHz to 1 mHz at 5 mV potentiostatic signal amplitude using a Solartron FRA 1250 frequency response analyzer and a Solartron model 1286 electrochemical interface. Before EIS measurements, the electrodes were left at open circuit for 15 min.

Results and Discussion

Performance of MH/MnO_2 FC.—Figure 2 shows the current-potential (I-E) performance of $LmNi_{4.1}Co_{0.4}Mn_{0.4}Al_{0.3}$/$MnO_2$ fuel cells measured by CV at 1.0 mV s^{-1} on H_2 and O_2 at 25°C. The performance of an AFC with Zetek (Geel, Belgium) electrodes (0.3 mg/cm^2 platinum on Vulcan XC-72 at both anode and cathode) is shown for comparison. The performance of MH/MnO_2 cells with electrocatalyst loadings of 150 mg/cm^2 was similar to that of the Zetek cell.

The addition of 0.5 wt % Pt into MH electrocatalyst decreased the hydrogen oxidation overpotential. When the loading was decreased from 100 mg/cm^2 to 60 mg/cm^2 (with 0.5 wt% Pt addition), the overpotential was relatively independent of electrocatalyst loading (Fig. 2). The electrocatalytic activity of MnO_2 electrodes with loadings in excess of 60 mg/cm^2 for oxygen reduction were comparable to that of electrodes with commercial Pt electrocatalyst, and their activity increased with loading.

MH and MnO_2 electrodes not only had a high catalytic activity for hydrogen oxidation and oxygen reduction, but also showed effective chemical energy storage. At the OCP or under continuous power output operation, the MH and MnO_2 electrodes are charged by hydrogen and oxygen. When the voltage was suddenly stepped from the OCP to a low voltage, a large additional current was supplied from the electrodes. Figure 3 shows the current as a function of time for MH containing 0.5 wt% Pt and MnO_2, both at 100 mg/cm^2 loading when the cell voltage was stepped from to OCP to 0.4 V. As expected, the dependence of current on time in Fig. 3 shows a typical battery performance under voltage step conditions. The current quickly decreased from an initial value of 180 to 125 mA/cm^2, and then slowly decreased to a steady-state current of

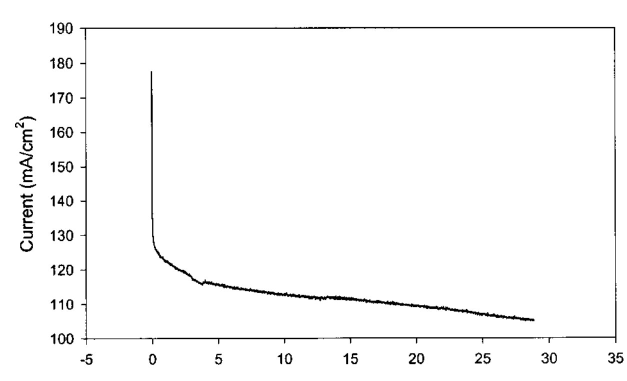

Figure 3. The dependence of current on time of a FC when cell voltage was stepped from open-circuit voltage to 0.4 V. Anode MH with 0.3 wt % Pt as Pt/C, cathode MnO_2. Catalyst loading 60 mg/cm^2 at both electrodes.

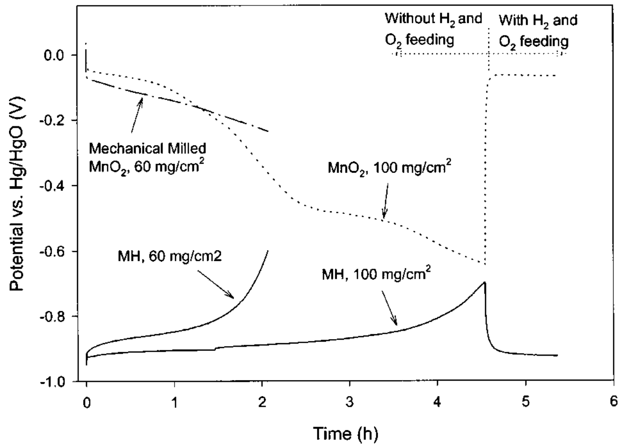

Figure 4. The potential behavior of MH/MnO_2 FC at a discharge current of 14 mA/cm^2 after H_2 and O_2 were shut off. For the AFC with 100 mg/cm^2 MH and MnO_2 loadings, H_2 and O_2 were supplied again when the potential of the MnO_2 cathode decreased to -0.7 V *vs.* Hg/HgO. The MnO_2 cathode with 60 mg/cm^2 loading was mechanically milled for 50 h.

around 100 mA/cm^2, which is close to the value determined by CV at 1.0 mV/s (Fig. 2) at the same cell voltage. The current in excess of 100 mA/cm^2 results from energy stored in the MH and MnO_2 electrodes. Therefore, incorporating the MH/MnO_2 battery element into an alkaline FC not only increased the continuous power output of the fuel cell (Fig. 2), but also enhanced its peak power output as is shown in Fig. 3.

Discharge performance of MH/MnO_2 FC with H_2 and O_2 interrupted.—When the H_2 and O_2 supplies are shut off, the cell continues to supply power as an MH/MnO_2 battery. Figure 4 shows the potential behavior of the $LmNi_{4.1}Co_{0.4}Mn_{0.4}Al_{0.3}$ and MnO_2 electrodes as a function of time at a discharge current of 14 mA/cm^2 under these conditions. H_2 and O_2 were resupplied to electrodes with 100 mg/cm^2 MH and MnO_2 loadings when the potential of the MnO_2 electrode had decreased to -0.7 V. Cathodes with 60 mg/cm^2 MnO_2 loadings prepared by mechanical milling for 50 h would operate for over 2 h, and those with 100 mg/cm^2 MH/MnO_2 loadings would operate for 4.5 h at 14 mA/cm^2. The capacities of the $LmNi_{4.1}Co_{0.4}Mn_{0.4}Al_{0.3}$ electrodes were 467 mAh/g at 60 mg/cm^2 loading and a mass current density of 233 mA/g (14 mA/cm^2) and 630 mAh/g at 100 mg/cm^2 loading at 140 mA/g (14 mA/cm^2). However, the capacity of the $LmNi_{4.1}Co_{0.4}Mn_{0.4}Al_{0.3}$ electrode was only about 250 mAh/g when measured as the anode for an MH/MnO_2 battery. The capacity in excess of 250 mAh/g for the $LmNi_{4.1}Co_{0.4}Mn_{0.4}Al_{0.3}$ AFC anode was due possibly to the large amount of hydrogen remaining in the channels and tube when the fuel is shut off. Similarly, the MnO_2 AFC cathode after the oxygen supply was shut off had a higher capacity than that (220 mAh/g) in the battery. Figure 4 also shows that the mechanically milled MnO_2 electrode had a higher catalytic activity than that of the original preparation, because it operated at higher potentials than those of the electrode without mechanical milling after 1.3 h of discharge.

Chargeability of MH and MnO_2 electrodes by fuel and oxidant.—MH and MnO_2 have both been successfully used as the rechargeable anode and cathode of an alkaline battery. It is also known that MH_x and MnO_x or MnO_2H_x can be respectively charged by gaseous H_2 and O_2. The chargeability of MH_x and MnO_x (MnO_2H_x) by H_2 and O_2 in a semi-wetted AFC electrocatalyst layer of FC required study. Figure 5 shows the cell voltage and electrode potential changes of MH and MnO_2 electrodes as a function of charging time by gaseous H_2 and O_2 after I-E measurement by CV

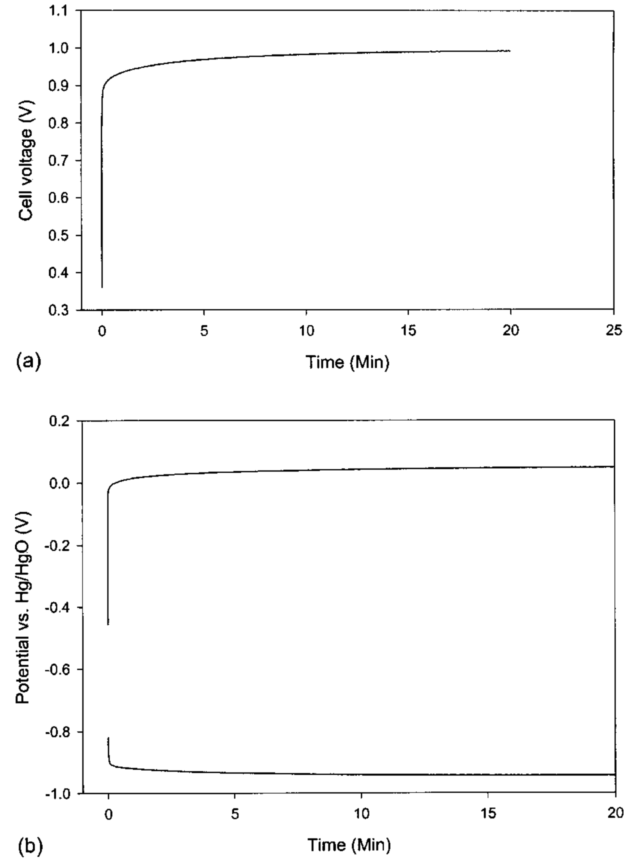

Figure 5. The (a) cell voltage and (b) potential changes of MH and MnO_2 anodes and cathodes as a function of recharging via reaction with gaseous H_2 and O_2 after I-E measurement by CV at 1.0 mV/s. MH and MnO_2 loadings 60 mg/cm^2.

at 1.0 mV/s. Both MH and MnO_2 electrodes in the FCs can be quickly recharged by H_2 and O_2 respectively, as is demonstrated by the rapid potential changes of both electrodes during exposure to the gases (Fig. 5b). The cell voltage increased with time and reached the equilibrium voltage of MH/MnO_2 cell after the gases were supplied for 20 min (Fig. 5a). Hence, a discharged MH/MnO_2 cell can be fully recharged in this time.

Charge/discharge performance of $LmNi_{4.1}Co_{0.4}Mn_{0.4}Al_{0.3}$ and MnO_2 as battery anode and cathode.—To compare the performance of MH/MnO_2 AFC after interruption of the supply of reactants with the battery behavior, the electrochemical charge/discharge properties of MH and MnO_2 electrode in 6 M KOH were investigated. Figure 6 shows the charge/discharge behavior and cycling performance of an $LmNi_{4.1}Co_{0.4}Mn_{0.4}Al_{0.3}$ anode under these conditions. As previously stated, the discharge capacity at 50 mA/g was around 250 mAh/g, which was much smaller than the discharge capacity of same electrode in the FC (Fig. 4). The change in potential as a function of discharge capacity (discharge time $\times$ 50 mA/g) under battery conditions (Fig. 6a) was similar to that of the same alloy under AFC conditions with no hydrogen supply (Fig. 4). The $LmNi_{4.1}Co_{0.4}Mn_{0.4}Al_{0.3}$ anode showed very stable charge/discharge behavior under battery conditions and did not require initial activation (Fig. 6b) because the material was mechanically milled for 30 min before electrode preparation.

Figure 7a shows the discharge/charge behavior of MnO_2 cathodes in 6 M KOH electrolytes at a cycling current of 50 mA/g. The discharge behavior of MnO_2 electrode shows two potential plateaus. The discharge capacity of MnO_2 electrode was *ca.* 220 mAh/g,

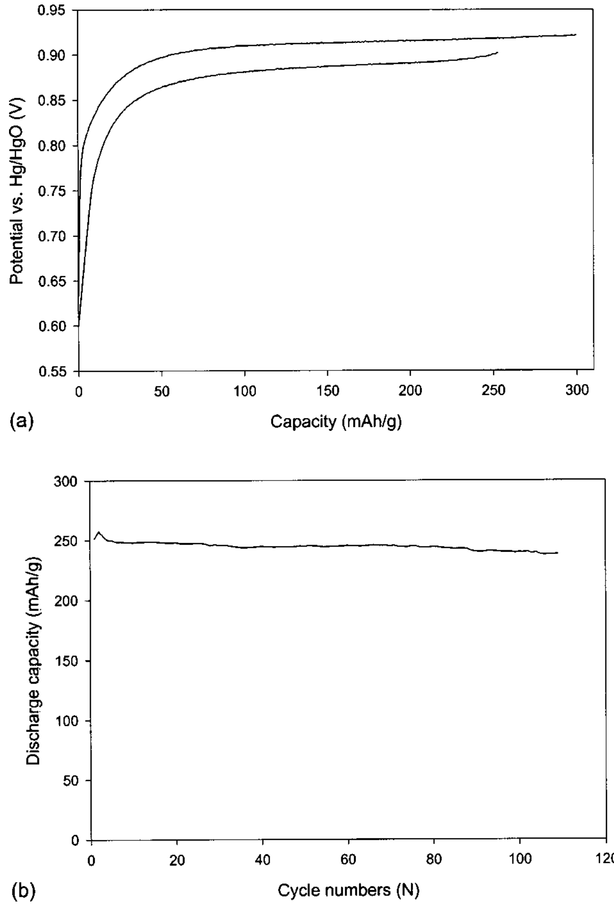

Figure 6. (a) The charge/discharge behavior and (b) cycling stability of MH anodes in alkaline electrolytes. The electrode was charged at 50 mA/g for 6.0 h and then discharged at 50 mA/g to −0.6 V *vs.* Hg/HgO.

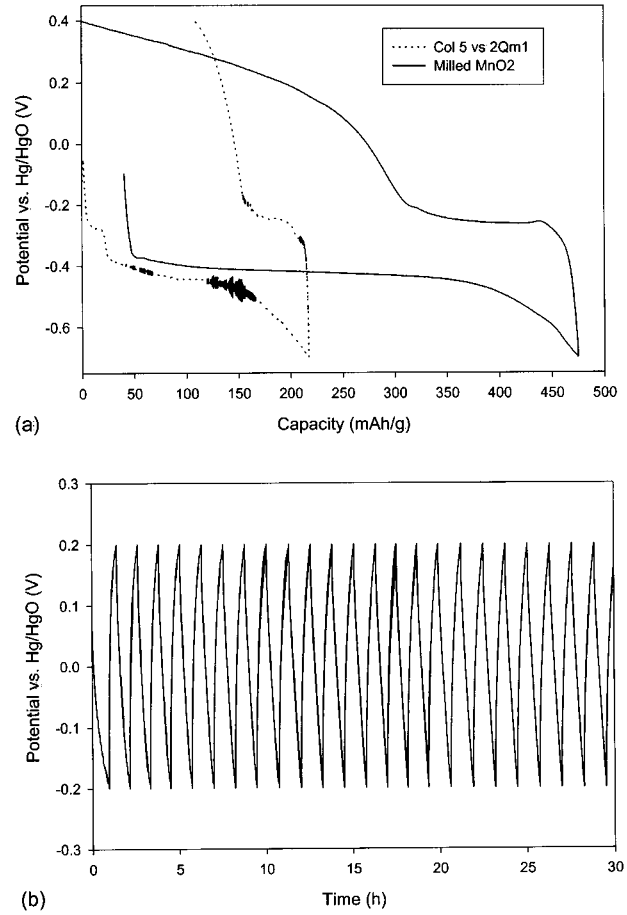

Figure 7. (a) The discharge/charge behavior of original and milled MnO_2 cathode cycling between +0.4 and −0.7 V in 6 M KOH electrolytes, and (b) cycling stability of milled MnO_2 cathode cycling between +0.2 and −0.2 V. Cycling current: 50 mA/g.

which was also much smaller than that of a same MnO_2 cathode with a 100 mg/cm^2 MnO_2 loading (630 mAh/g) under AFC conditions with no oxygen supply (Fig. 4). The capacity of the MnO_2 cathode under FC conditions (Fig. 4) at potentials below −0.4 V was similar to that of similar MnO_2 cathodes under battery conditions (Fig. 7a). Therefore, the capacity of MnO_2 cathode at potential around −0.1 V under AFC conditions with no oxygen supply (Fig. 4) was due possibly to the large amount of oxygen remaining in the channels and tube when the oxygen is shut off.

To fully use the energy stored in MnO_2, the AFC cathode should normally operate at potentials slightly above that of the MnO_2 plateau, allowing it to go below the plateau when high power output is needed. If the normal operating voltage of the FC is 0.6 V, and potential of MH anode is at −0.8 to −0.85 V (Hg/HgO), the plateau potential of cathode around −0.2 to −0.25 V (Hg/HgO). However, the actual MnO_2 plateau potential is about −0.4 V (Hg/HgO). Modifying MnO_2 by doping or by mixing it with small amounts of $Ni(OH)_2$ can increase its plateau potential. However, incorporation of 10 wt% $Ni(OH)_2$ was shown to decrease the electrocatalytic activity for oxygen reduction.

Figure 7a shows that mechanically milled MnO_2 had a much higher battery capacity than that of the original preparation, indicating that breakdown of large agglomerates and intimate mixing resulted in an improved conduction pathway distribution between graphite and MnO_2,[7] giving higher overall electrochemical kinetics. Mechanically milling graphite is known to produce a more disordered carbon, so crystalline MnO_2 may result in an amorphous phase with increased ability to absorb protons and higher electrocatalytic activity for oxygen reduction.[8] In addition, mechanically-milled MnO_2 has higher charge/discharge cycling stability because the improved conduction pathways between it and graphite are effective in suppressing the formation of electrochemically inactive Mn_3O_4 under deep discharge conditions.[7] Accumulation of Mn_3O_4 during repeated charge/discharge cycling causes capacity decline of the MnO_2 cathode. Although the addition of bismuth oxide can effectively suppress Mn_3O_4 formation and increase the cycling stability of MnO_2 in alkaline electrolytes, slightly soluble bismuthite ion may move to the anode where it may be deposited as bismuth, decreasing the electrocatalytic activity of MH for hydrogen absorption. A mechanically milled bismuth-free MnO_2 AFC cathode showed a reasonable cycling stability because it normally operated in the potential range between −0.1 to −0.4 V (Hg/HgO), higher than the Mn_3O_4 formation of −0.5 V (Hg/HgO).[7] Figure 7b shows the excellent cycling stability of mechanically milled MnO_2 during charge/discharge cycling between +0.2 and −0.2 V (Hg/HgO). However, the potential of the MnO_2 cathode may decrease below −0.5 V at very high peak power demands, which could result in possible formation of Mn_3O_4 and would concurrently result in a low cycling stability. In this case, a separate Ni/MH or Li-ion battery may still provide better power assistance to the FC, as both devices are optimized.

EIS measurement of MH/MnO_2 and Pt AFCs.—The MH/MnO_2 FC can be considered as a combination of a conventional AFC and a MH/MnO_2 secondary cell. These differences can be quantified by electrochemical impedance spectroscopy. Figure 8 shows the imped-

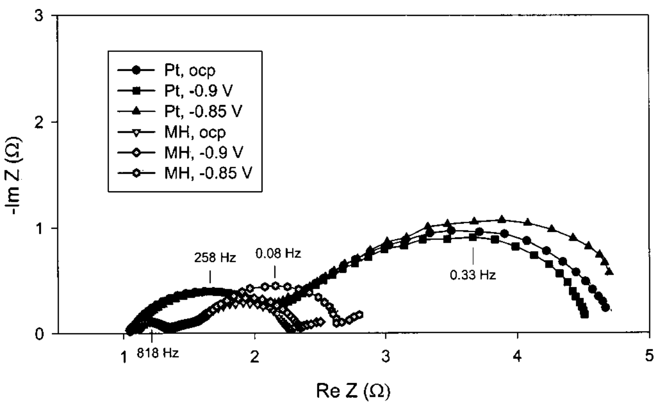

Figure 8. Impedance spectra of MH and Pt AFC anodes at different potentials. Frequencies indicated in plots. MH anode loading: 60 mg/cm^2 + 0.3 mg/cm^2 Pt, Pt catalyst loading: 0.3 mg/cm^2.

ances of Pt and MH anodes as a function of potential in H_2/O_2 AFCs, and Fig. 9 shows similar data for Pt and MnO_2 cathodes. The catalyst loadings at both the anode and cathode were 0.3 g/cm^2 (Pt) and 60 mg/cm^2 (MH/MnO_2), respectively, with 0.3 mg/cm^2 Pt in the MH anode electrocatalyst. The impedance diagram for hydrogen oxidation on both Pt and MH anode (Fig. 8) consists of two suppressed semicircles, with an additional Warburg diffusion slope *W* for MH. The semicircle in the low-frequency range, which was potential dependent, was attributed to the charge transfer reaction, while the semicircle in the high frequency region results from the impedances in series for electron transfer and hydrogen transfer between the absorbed and the adsorbed state for MH.[9] The Warburg slope in the low-frequency region for MH was due to hydrogen diffusion into the MH particles. No Warburg slope was seen for the Pt anode, because Pt metal does not absorb hydrogen. The impedance of MH at the above loadings was only half of the Pt electrocatalyst at 0.3 mg/cm^2 loading. The fact that the high-frequency semicircle diameter for MH is smaller than that for Pt impedance may be a result of the higher electronic conductivity of MH + graphite mixture than for carbon decorated with small amounts of Pt. The small diameter of the low-frequency MH semicircle was attributed to the high MH loading (60 mg/cm^2), which greatly decreased charge-transfer resistance. The higher current at the MH anode than that at Pt (Fig. 2) may be attributed to its high electronic conductivity and the higher activity of the MH + Pt/graphite electrocatalyst.

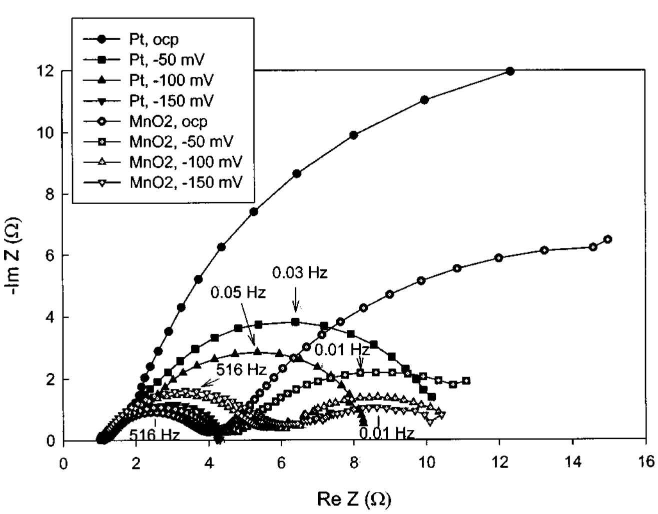

Figure 9. Impedance spectra of MnO_2 and Pt AFC cathodes at different potentials. The numbers in the plots indicate the frequency. MnO_2 loading: 60 mg/cm^2. Pt loading, as Fig. 8.

The oxygen reduction impedance on the Pt cathode also shows two suppressed semicircles. The diameter of the second (at low frequency) decreased rapidly with increasing overpotential (Fig. 9). As for hydrogen oxidation on Pt, it may be attributed to oxygen reduction charge transfer on the Pt electrocatalyst. Because the charge-transfer impedance was large at low overpotentials (<150 mV), the high-frequency semicircle for the series electrode impedance of and the low-frequency semicircle for diffusion of species involved in oxygen reduction were masked by the large value of the charge-transfer impedance. It is well known that carbon surfaces are quite active for oxygen reduction in the AFC, and that low platinum loadings enhance this activity.[10]

The charge-transfer impedance of the MnO_2 electrode with state loading was similar to that of the Pt cathode with 0.3 mg/cm^2 loading when the electrode potential was higher than −0.150 V. However the high-frequency semicircle for MnO_2 was larger than that for Pt, which may possibly be attributed to the high loading of MnO_2, a poor electronic conductor. Increasing the electronic conductivity of the MnO_2 cathode is expected to improve its electrochemical performance for oxygen reduction.

Conclusions

MH alloy (MH, $LmNi_{4.1}Co_{0.4}Mn_{0.4}Al_{0.3}$) and MnO_2 have been used successfully as electrocatalysts for hydrogen oxidation and oxygen reduction in an AFC. Its steady-state power output with high catalyst loading (>150 mg/cm^2 at anode and cathode) was comparable to that of carbon-supported platinum AFC with 0.3 mg/cm^2 loading at the anode and cathode. However, the MH/MnO_2 AFC delivered additional power when the cell voltage was stepped from normal operation voltage to a lower value because MH and MnO_2 not only act as electrocatalysts but also as energy storage as in a secondary cell. The MH and MnO_2 anode and cathode were quickly recharged by gaseous hydrogen and oxygen. During charging, the cell voltage returned to its normal value. Other advantages of the MH/MnO_2 AFC are its potentially low cost and the fact that it can deliver a certain amount of energy even after the hydrogen and oxygen supply has been shut off. Mixing a small amount of Pt electrocatalyst into the MH material can eliminate the usual activation process of MH anode activation process, and further improve hydrogen oxidation electrocatalysis.

Lamar University assisted in meeting the publication costs of this article.

References

1. S. Lee, J. Kim, H. Lee, P. Lee, and J. Lee, *J. Electrochem. Soc.*, **149**, A603 (2002).
2. D. Chartouni, N. Kuriyama, T. Kiyobayashi, and J. Chen, *Int. J. Hydrogen Energy*, **27**, 945 (2002).
3. X. Wang, Y. Chen, H. Pan, R. Xu, S. Li, L. Chen, C. Chen, and Q. Wang, *J. Alloys Compd.*, **293-295**, 833 (1999).
4. B. Klapste, J. Vondrak, and J. Velicka, *Electrochim. Acta*, **47**, 2365 (2002).
5. X. Xia and Z. Guo, *J. Electrochem. Soc.*, **144**, L213 (1997).
6. X. Xia, C. Zhang, Z. Guo, H. K. Liu, and G. Walter, *J. Power Sources*, **109**, 11 (2002).
7. D. Im and A. Manthiram, *J. Electrochem. Soc.*, **150**, A68 (2003).
8. J. Yang and J. J. Xu, *Electrochem. Commun.*, In press.
9. C. Wang, A. Rakotondrainibe, A. J. Appleby, and F. E. Little, *J. Electrochem. Soc.*, **147**, 4432 (2000).
10. A. J. Appleby and F. R. Foulkes, *Fuel Cell Handbook*, Van Nostrand Reinhold, New York (1992).